

Phase transition and electronic state modification by lattice strain in 0.5-monolayer Sn/Cu(001)

Koichiro Yaji, Yuki Nara, Kan Nakatsuji, Takushi Iimori, Kazuma Yagyū, Ryuichi Nakayama, Naoki Nemoto, and Fumio Komori

Institute for Solid State Physics, The University of Tokyo, Kashiwashi, Chiba 277-8581, Japan

(Received 24 August 2007; revised manuscript received 16 April 2008; published 16 July 2008)

We have studied the phase transition of 0.5-monolayer (ML) of Sn-adsorbed Cu(001) surface between $(\sqrt{2} \times \sqrt{2})R45^\circ$ structure at high-temperature phase and $(3\sqrt{2} \times \sqrt{2})R45^\circ$ structure at low-temperature phase, which was previously attributed to a charge-density wave (CDW) formation. The $(3\sqrt{2} \times \sqrt{2})R45^\circ$ superstructure was found in a very small area ($\sim 3 \times 3$ nm²). This result disagrees with the predictions by both the weak- and the strong-coupling CDWs with long coherence. In addition, the observed gap energy and the CDW gap extending in reciprocal space for the surface resonance band are inconsistent with the strong-coupling CDW with short coherence. Modification of this band of 0.5 ML Sn/Cu(001) by the lattice compression is studied by means of N adsorption. The band shifts to the higher-energy side with compressive strain field.

DOI: 10.1103/PhysRevB.78.035427

PACS number(s): 68.35.Rh, 73.20.At, 64.70.-p

I. INTRODUCTION

Phase transition in low-dimensional materials has attracted much attention because of its peculiar properties compared with those in bulk materials. One of the typical examples is the charge-density wave (CDW) caused by the electron-phonon interaction. A low-dimensional metallic state is unstable because of this interaction, and the charge is periodically modulated in the CDW ground state.¹⁻³ For an ideal one-dimensional system, Fermi-surface nesting is always perfect, and the system can be led to the CDW transition. On the other hand, concerning two-dimensional systems such as solid surfaces, there have been a number of arguments on whether CDW drives the phase transition or not. The type of CDW strongly depends on the strength of electron-phonon coupling.⁴ In the case of weak-coupling, CDW is accompanied by the displacement of atoms, and the CDW correlation length is much longer than the CDW period. On the other hand, strong-coupling CDW is characterized by a wide band gap and a short CDW correlation length.

Structural phase transition and electronic states for elements of groups 13 and 14 of the Periodic Table (In, Sn, and Tl) adsorbed on the Cu(001) surface have been studied both experimentally and theoretically.⁴⁻⁷ In particular, a correlation was pointed out between the structural phase transition and the opening of the energy gap in the electronic band structure around Fermi level (E_F). Thus the phase transition is interpreted as the CDW formation due to the electron-phonon interaction with Fermi-surface nesting. For In and Sn on Cu(001), Aruga⁴ suggested that the CDW transition for these surfaces is classified into a new category with a strong coupling and a long CDW correlation length.

Here, we focus on the Cu(001) surface with 0.5-monolayer (ML) of Sn on average [0.5-ML Sn/Cu(001)], which exhibits a reversible phase transition between a $(\sqrt{2} \times \sqrt{2})R45^\circ$ phase [high-temperature (HT) phase] and a $(3\sqrt{2} \times \sqrt{2})R45^\circ$ phase [low-temperature (LT) phase] at 360 K accompanied with a gap formation of the electronic states at E_F .^{5,8-11} Martínez-Blanco *et al.*⁵ claimed that a CDW formation with Fermi-surface nesting of a surface resonance band is a trigger of the phase transition on the basis of their

results by angle-resolved photoemission spectroscopy (ARPES). The observed critical temperature T_C of the electronic system is 360 K and the gap energy below Fermi level is ~ 0.7 eV at LT phase. In the Peierls theory of weak-coupling CDW, the gap energy Δ is described by the formula $\Delta = 1.76k_B T_C$.^{1,2} However, the observed value of Δ is much larger than that estimated from the observed T_C using this formula. Furthermore, the CDW-folding point of the surface resonance band deviates $\sim 8\%$ from a nesting vector $2k_F$, where k_F denotes Fermi wave number. These suggest strong-coupling CDW or another mechanism as an origin of the observed structural transition. The ordering of the surface lattice would make an energy gap in the electronic band at the new boundary of the surface Brillouin zone (SBZ). In the CDW picture, there is another difficulty in how to make an ordered $(\sqrt{2} \times \sqrt{2})R45^\circ$ structure from the $(3\sqrt{2} \times \sqrt{2})R45^\circ$ one with a missing row of Cu atoms at the surface.¹⁰

When we modify the lattice constant of the surface, we can expect changes in both the lattice vibration and the electronic states. These would largely affect the structural phase transition at the surface especially when the electron-phonon coupling is important. It is interesting to study how the change in the electronic states due to the phase transition is modified by lattice compression. This will give significant information on the phase transition. Previously, it was shown that the electronic states of the clean Cu(001) surface change with the lattice compression due to nitrogen adsorption.^{12,13} On a partially N-adsorbed surface, $c(2 \times 2)$ -N domains are formed and coexist with clean Cu surface.¹⁴ The surface lattice of the $c(2 \times 2)$ -N domain is slightly expanded from that of the wide clean Cu surface, and thus the lattice of the coexisting clean surface is slightly compressed.¹⁵⁻¹⁷

In the present study, we have investigated the phase transition of 0.5-ML Sn/Cu(001) surface by scanning tunneling microscopy (STM), ARPES, and Sn *4d* core-level spectroscopy to make clear whether the transition is interpreted as the CDW scenario. In the STM experiment, we used N-adsorbed Cu(001) surfaces to restrict the domain size of the 0.5-ML Sn/Cu(001) surface to less than 10 nm². The CDW with a correlation length larger than the domain size would be unstable in such a small area. The results of the STM observa-

tion are inconsistent with the both weak- and strong-coupling CDW with long coherence. The strong-coupling CDW with short coherence cannot explain the observed gap extending for δk in reciprocal space (0.1 \AA^{-1}) and the gap energy (0.7 eV). We have also studied the change in the surface resonance band by the lattice compression with N adsorption. The band shifts to the higher-energy side with the lattice compression. This behavior is similar to that of a Cu $4sp$ surface state of the clean Cu(001) surface.¹³

II. EXPERIMENT

The substrate clean Cu surface was obtained by several cycles of 1 keV Ar^+ -ion bombardment and subsequent annealing up to 870 K in a few minutes. The N-adsorbed Cu(001) surface was prepared by N^+ -ion bombardment with the beam energy of 500 eV at room temperature (RT), where the N_2 pressure was 1.0×10^{-5} Torr. Subsequently, the sample was annealed at 470 K for 5 min to make an ordered $c(2 \times 2)$ arrangement. Tin was then deposited onto the surface kept at RT from an alumina crucible heated with a tantalum filament. Surface structures were observed using STM (Omicron, Micro-STM) in an ultrahigh vacuum chamber at RT. The ARPES spectra were measured using an angular mode of a hemispherical electron energy analyzer (VG Scienta SES2002 and SES100). Unpolarized He I ($h\nu = 21.22$ eV) and He II ($h\nu = 40.82$ eV) radiations were used as photon sources for ARPES measurement. We also measured the Sn $4d$ core-level spectra at the beamline 18A (BL18A) of a synchrotron radiation facility (KEK-PF) using 55 eV photons. The incident angle of the photon was 45° , and the spectra were taken at grazing emission (60°) with respect to the surface normal.

III. RESULTS AND DISCUSSION

A. Structure

Figure 1(a) is an STM image of the 0.5-ML Sn/Cu(001) surface. Parts of the surface Cu atoms are replaced by Sn atoms. The surface shows a $(3\sqrt{2} \times \sqrt{2})R45^\circ$ periodicity, which agrees with a former report.¹⁰ The protrusions are assigned as surface Sn atoms, and Cu atoms cannot be recognized in the image. Two domains coexist on this surface, and the detailed results on the Sn-adsorbed surfaces by STM were described elsewhere.¹¹

Figure 2 exhibits an STM image of Sn-adsorbed 0.3-ML N/Cu(001) surface. A very narrow $(3\sqrt{2} \times \sqrt{2})R45^\circ$ area ($\sim 3 \times 3 \text{ nm}^2$), named B, can be recognized. Domains A are $c(2 \times 2)$ -N/Cu(001), and B is a local 0.5-ML Sn/Cu(001) region. The rectangle denotes the unit cell of the $(3\sqrt{2} \times \sqrt{2})R45^\circ$ structure. The other areas have 3/8-ML Sn/Cu(001) surface, which is another phase as reported in Ref. 11. Only 1~2 periods (1~2 nm) of the $3\sqrt{2}$ structure exist within the area.

B. Electronic state

We measured photoemission spectra at $h\nu = 21.22$ eV along line A in $\bar{\Gamma}\bar{M}$ direction as shown in Fig. 3(a). The

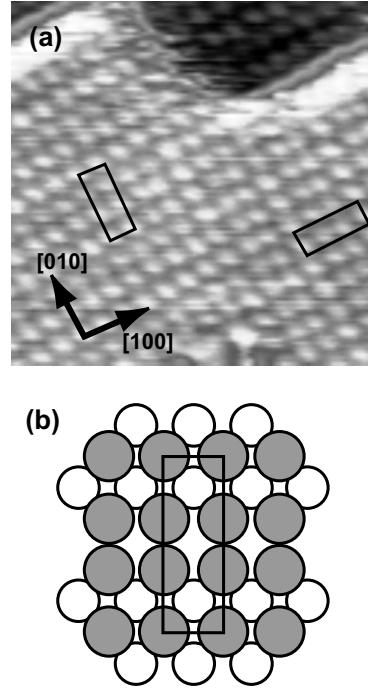


FIG. 1. (a) STM image ($5 \times 5 \text{ nm}^2$) of the Cu(001) surface covered with 0.5 ML of Sn on average. The rectangles in the STM image denote the unit cells of $(3\sqrt{2} \times \sqrt{2})R45^\circ$ phase in two different domains. (b) Schematic ball model of the surface structure. The gray and white circles denote Sn and Cu atoms, respectively.

results for 0.5-ML Sn/Cu(001) are given in Fig. 3(b). Here, the average coverage of Sn was confirmed by observing the $(3\sqrt{2} \times \sqrt{2})R45^\circ$ low-energy electron-diffraction (LEED) spots. The binding energy versus momentum (E - k) curves can be drawn from the photoemission spectra as shown in Fig. 3(c) using the following formula: $k_{\parallel} = 0.512\sqrt{(h\nu - E_B - E_W)}$, where E_B is the binding energy and E_W is the work function of the sample. The latter was experimentally obtained from the cut-off energy of secondary photoelectrons. Two dispersive bands named S_1 and S_2 are seen because of the existence of two domains as in the former report.⁵ These bands are ascribed to the sp -like surface resonance bands.^{4,5} The S_1 band, which behaves as in the $\sqrt{2}$

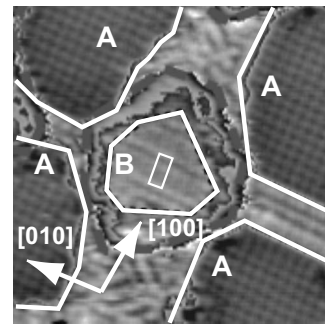


FIG. 2. STM image ($10 \times 10 \text{ nm}^2$) of Sn/N/Cu(001) surface. Domains A are $c(2 \times 2)$ N/Cu(001), and B is a local 0.5-ML Sn/Cu(001) region. The rectangle in the domain B denotes the unit cell of $(3\sqrt{2} \times \sqrt{2})R45^\circ$ structure. The other areas have 3/8-ML Sn/Cu(001) surface, which is another phase as observed in Ref. 11.

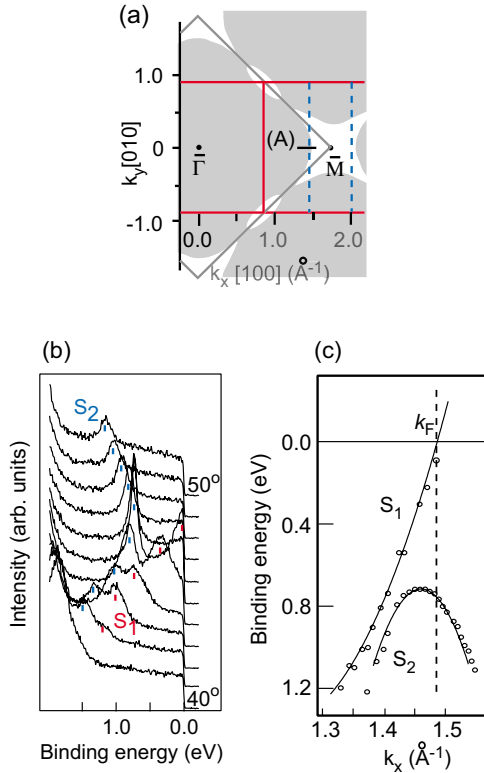


FIG. 3. (Color online) (a) SBZ for 1×1 (gray line), $(\sqrt{2} \times \sqrt{2})R45^\circ$ (solid line), and $(3\sqrt{2} \times \sqrt{2})R45^\circ$ (dashed line). The unshaded areas denote the bulk band gaps. (b) ARPES spectra for 0.5-ML Sn/Cu(001) surfaces. (c) Surface S_1 and S_2 band dispersion for 0.5-ML Sn/Cu(001) . The symbols show the experimental data and the solid lines are fitting results by a simple one-band model with parabolic dispersion. The dashed lines are guides for the position of k_F .

phase and is observed similarly in the HT phase,⁵ crosses the Fermi level. On the other hand, the S_2 band, which is observed only in the LT phase, folds back at ~ 0.7 eV below E_F .

C. Comparison with CDW scenario

First, we exclude the CDW with a long correlation length as an origin of the phase transition. As shown in Fig. 2, the $(3\sqrt{2} \times \sqrt{2})R45^\circ$ superstructure is made even in a region as small as $3 \times 3 \text{ nm}^2$. The result indicates the correlation length (ξ_{CDW}) to be as short as 2 nm. Thus, the observed superstructure cannot be explained by both the weak- and the strong-coupling CDWs with a long correlation length. Moreover, in such a small area, we further consider the quantization of the electronic states in S_2 band. The estimated electron-level separation can exceed the energy gap of S_2 band, and thus, the gap formation due to the CDW formation little helps to reduce the total free energy. The weak-coupling CDW picture is inconsistent with the observation shown in Fig. 3(c) because the wave number at the band-folding point of the S_2 band deviates from the k_F of the S_1 band.

Second, we discuss another possible CDW with a strong electron-phonon coupling and a short correlation length.

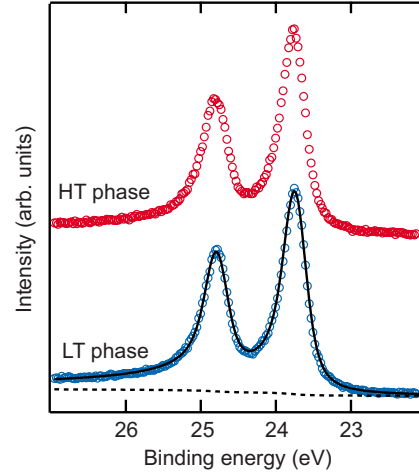


FIG. 4. (Color online) Sn $4d$ core-level spectra for 0.5-ML Sn/Cu(001) at HT and LT phases. The circular plots are data points and the solid line is fitting result. The dashed curve is the background function used in fitting process.

Here, a gap extending for δk in reciprocal space is estimated from the structure in the small area by $2\pi/\xi_{\text{CDW}}$. If the $(3\sqrt{2} \times \sqrt{2})R45^\circ$ structure is interpreted as the strong-coupling CDW with a correlation length ξ_{CDW} as short as ~ 2 nm, the gap extending in reciprocal space and the top of the S_2 band should be more than 0.3 \AA^{-1} and 2 eV below E_F , respectively. These values are much larger than the observed extending gap (0.1 \AA^{-1}) and the top energy (0.7 eV) of S_2 band by means of ARPES in Fig. 3(c). Thus, the phase transition cannot be explained by the CDW scenario of this type.

All the above experimental results imply that the phase transition from LT phase to HT phase of 0.5-ML Sn/Cu(001) surface cannot be attributed to the existing CDW mechanisms. It is considered that the band merely folds back at the Brillouin-zone edge of LT phase. It is well known that the band can fold back at the Brillouin-zone edge even if there is no CDW in the system.

D. Results of core-level spectroscopy and type of phase transition

Figure 4 shows the Sn $4d$ core level at both HT and LT phases. The photon energy was set to 55 eV. The Sn $4d_{5/2}$ and $4d_{3/2}$ peaks are located at 23.7 and 24.8 eV below Fermi level, respectively. The core-level spectrum at the LT phase was fitted by a Voigt function with a single component. The best fitting result is shown by a solid line, in which the spectrum is broadened by the Lorentzian and Gaussian functions with the full width at half maximum (FWHM) of 0.21 ± 0.01 and 0.22 ± 0.01 eV. Here, the value of the FWHM of Gaussian function is consistent with the energy resolution of the apparatus. The fitting result of HT phase is the same as that of LT phase within the error of the experiments. There is no detectable shift of the core-energy level and there is little change in the line shape in the spectra between LT and HT phases. These indicate that the chemical bonding state is not influenced by the structural phase transition between HT

phase and LT phase. This result is consistent with the above conclusion that the structural phase transition is not linked to the formation of a charge-density modulation. We note that to interpret the result using the CDW scenario, we should take the core-level shift due to the CDW formation to be less than 50 meV. Otherwise, we could detect a change in the spectrum shape.

One of the possible mechanisms of the phase transition in the 0.5-ML Sn/Cu(001) surface is an *order-disorder* transition with a lack of long-range order in the $(3\sqrt{2} \times \sqrt{2})R45^\circ$ periodicity due to thermal effect. Here, the $(3\sqrt{2} \times \sqrt{2})R45^\circ$ surface at LT phase is an ordered surface and the $(\sqrt{2} \times \sqrt{2})R45^\circ$ surface at HT phase is a disordered one. It is noted that the ordered $(\sqrt{2} \times \sqrt{2})R45^\circ$ structure cannot be formed by a continuous movement of the surface Sn and Cu atoms in the ordered $(3\sqrt{2} \times \sqrt{2})R45^\circ$ structure because the $(3\sqrt{2} \times \sqrt{2})R45^\circ$ structure includes a missing row of the surface Cu atoms.¹⁰ Thus, the possible structure in HT phase is that the missing rows of the surface Cu atoms are disordered to maintain the local structure of the surface Sn and Cu atoms almost the same as that in LT phase. For the core-level spectrum, the line shape is not influenced by the *order-disorder* phase transition because the time scale of the photoelectron emission process is much shorter than that of the thermal fluctuation of the structure. On the other hand, the absence of the extra $(3\sqrt{2} \times \sqrt{2})R45^\circ$ spots in the low-energy electron diffraction and surface x-ray diffraction at HT phase, which were shown in Ref. 5, can be explained as the lack of the long-range order of the missing row with thermal fluctuation.

Similar surface resonance bands were reported for In-adsorbed Cu(001) surfaces. Submonolayer In on the Cu(001) surface shows a structural phase transition at around 400 K, where the dispersion of the surface resonance band is very similar to that of Sn/Cu(001). Moreover, only a small region of the Fermi surface satisfies the nesting condition as in Sn/Cu(001). So far, the phase transition has been classified into the strong-coupling CDW with a long CDW correlation length.⁴ However, the above experimental results suggest that the *order-disorder* transition without CDW has to be considered as a candidate for the transition mechanism as well as the 0.5-ML Sn/Cu(001) system.

E. Band modification by lattice compression

In this subsection, we discuss the energy shift of the resonance band on the partially N-covered surface. Figures 5(a) and 5(b) show STM images of the 0.1-ML N-adsorbed Cu(001) surface and 0.45 ML of Sn deposited on 0.05-ML N-adsorbed Cu(001) surface on average at RT, respectively. Hereafter, we abbreviate the former as 0.1-ML N/Cu(001) and the latter as 0.45-ML Sn/0.05-ML N/Cu(001).

The dark areas in Figs. 5(a) and 5(b) are the $c(2 \times 2)$ -N/Cu(001) domains, and the bright areas are the clean Cu(001) and Sn/Cu(001) surfaces, respectively. The clean Cu regions in Fig. 5(a) are compressed by the N adsorption as detected by ARPES.^{12,13} It was previously demonstrated that noble and magnetic transition-metal atoms do not adsorb on the N/Cu(001) domains at RT when they are deposited on the

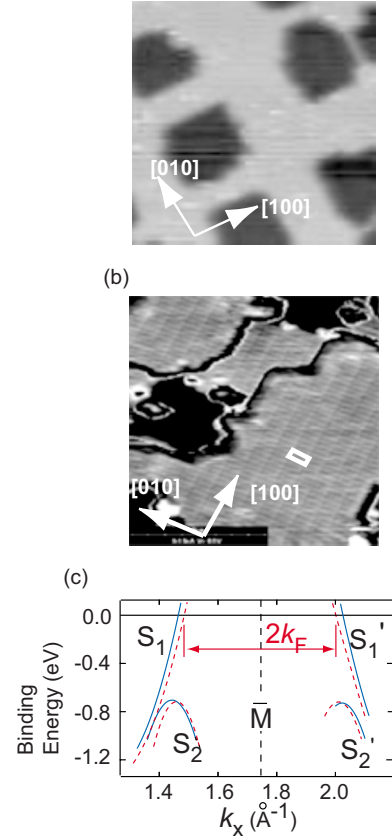


FIG. 5. (Color online) (a) STM image (15×15 nm²) of 0.1-ML N-adsorbed Cu(001) surface. The dark areas are $c(2 \times 2)$ -N/Cu(001) domains. The bright area is the clean Cu surface. (b) STM image (15×15 nm²) for 0.45-ML Sn/0.05-ML N/Cu(001) surface. The dark areas are $c(2 \times 2)$ -N/Cu(001) domains. The bright areas are 0.5-ML Sn/Cu regions. (c) The equivalent band structures beyond \bar{M} point for 0.5-ML Sn/ (dashed line) and 0.45-ML Sn/0.05-ML N/Cu(001) (solid line).

partially N-adsorbed Cu(001) surface with a slow deposition rate.¹⁸ The attractive force between these atoms and the N-adsorbed surface is so weak that the atoms diffuse to the clean Cu surface at least just after the deposition. We confirmed by a number of STM images that the Sn atoms also adsorb exclusively on the clean Cu area of N/Cu(001). On the N-adsorbed area, the $c(2 \times 2)$ -N/Cu(001) structure was clearly observed by STM even after the Sn deposition. Thus, we can easily adjust the density of Sn atoms on the clean surface to be 0.5 ML. On 0.45-ML Sn/0.05-ML N/Cu(001), the Sn-adsorbed Cu(001) area has the $(3\sqrt{2} \times \sqrt{2})R45^\circ$ structure at RT as shown in Fig. 5(b), indicating the formation of LT phase. Because of the coexisting $c(2 \times 2)$ -N/Cu(001) domains, the lattice of the LT-phase areas is compressed.

The E - k curves are shown in Fig. 5(c). The dashed and solid lines correspond to the bands for 0.5-ML Sn and 0.45-ML Sn/0.05-ML N/Cu(001), respectively. The k_F of S_1 band and the band-folding point of S_2 band between $\bar{\Gamma}$ and \bar{M} for 0.45-ML Sn/0.05-ML N/Cu(001) shift to the lower-wave-number side compared with those for 0.5-ML Sn/Cu(001). On the other hand, for the equivalent bands (S'_1 and

S_2') beyond the \bar{M} point, the k_F' and the folding point shift to the higher-wave-number side. This is opposite to the behavior expected in the case that both bands shift to momentum direction with the modification of SBZ by the lattice compression. In this case, the k_F and k_F' should shift to the same direction. We notice that the \bar{M} point, which can be determined from the middle of the k_F and k_F' , shows no shift by the N adsorption within the experimental accuracy. This means that the modification of the lattice constant for the Sn/Cu area was not detectable as the momentum shift of the electronic states. Thus, we conclude that the S_1 (S_1') band shifts to the higher-energy side, not to the higher- or lower-wave-number side. The energy of the sp -derived band largely changes with the compressive strain potential. Sekiba *et al.*¹³ reported that a Cu $4sp$ surface state of the clean Cu(001) surface shifts to the energy direction by the similar small amount of N-atom adsorption.

We can exclude the influence of the possible coexisting impurity surface phases because of the error in the amount of Sn in the results of ARPES in the following way: If a minor fraction of Sn atoms is adsorbed on N-covered parts of the surface, 3/8-ML Sn/Cu(001) phase would coexist with 0.5-ML Sn phase in the Sn/Cu area as seen in Ref. 11. However, as described in the Appendix, the energy dispersion of the resonance band in 3/8-ML Sn/Cu phase can be clearly discriminated from that of 0.5-ML Sn/Cu phase; the difference in the dispersion between them is larger than the band modification induced by the compressed strain field. Thus, it is considered that the influence on the electronic band structure is negligible at both HT and LT phases even if there are a small fraction of Sn atoms on the $c(2 \times 2)$ -N patch. When the total amount of local Sn density is larger than 0.5 ML, the 5/8-ML Sn/Cu(001) phase coexists with the 0.5-ML Sn/Cu(001) phase. In this case, however, there is no detectable electronic band from the 5/8-ML Sn/Cu(001) phase in this E - k region, and the influence on the electronic band structure is again negligible at both HT and LT phases.

The STM observation of 0.45-ML Sn/0.05-ML N/Cu(001) surface confirmed the formation of the $(3\sqrt{2} \times \sqrt{2})R45^\circ$ -Sn alloy structure. The k_F and the band-folding points of S_2 band for 0.45-ML Sn/0.05-ML N/Cu(001) shift to the lower-wave-number side compared with those for 0.5-ML Sn/Cu(001). On the other hand, the modification of SBZ is not detectable. Here we can assume that the k_F in LT phase is the same as k_F in HT phase because this is the case on the surface without N adsorption.⁵ Then, the nesting vector become $\sim 7\%$ larger than 1/3 of the $(\sqrt{2} \times \sqrt{2})R45^\circ$ reciprocal-lattice vector on the nitrogen-modified surfaces. This means that 0.5-ML Sn/Cu(001) area forms the $(3\sqrt{2} \times \sqrt{2})R45^\circ$ periodicity even if the exact condition of the Fermi-surface nesting is broken. Thus, this result using the compressive strain field supports that the exact Fermi-surface nesting is not the required condition for the structural phase transition between the $(\sqrt{2} \times \sqrt{2})R45^\circ$ -Sn and $(3\sqrt{2} \times \sqrt{2})R45^\circ$ -Sn structures. Here, we note that this is inconsistent with the weak-coupling CDW scenario, which is sensitive to the nesting condition.

IV. CONCLUSION

We have studied the phase transition of the 0.5-ML Sn/Cu(001) surface using STM, ARPES, and Sn $4d$ core-level

spectra. In the STM observation, a very small region with the $(3\sqrt{2} \times \sqrt{2})R45^\circ$ structure of the 0.5-ML Sn/Cu(001) was found at RT. This result disagrees with the predictions by the both weak- and the strong-coupling CDWs with long coherence. The strong-coupling CDW with short coherence cannot explain the observed gap extending in reciprocal space (0.1 \AA^{-1}) and the gap energy (0.7 eV) which are evaluated from the band structure shown in Fig. 3(c). We have suggested that the possible mechanism of the phase transition is the *order-disorder* one instead of the previously assigned CDW transition on the basis of the structure of LT phase with a missing Cu row. In HT phase, the missing row should be disordered. We have also studied the Sn $4d$ spectra and the change in the surface resonance band of 0.5-ML Sn/Cu(001) surface by the lattice compression. The observed Sn $4d$ spectra are independent of the phase transition. The k_F of the surface resonance band S_1 in LT phase shifts to the higher-energy side with compressive strain field. The folding point of the S_2 band in LT phase shift to the lower-wave-number side. If it is the same as the k_F in HT phase, the exact nesting condition of the Fermi surface for the weak coupling with long coherence CDW scenario is broken. These are consistent with the above conclusion on the phase transition.

Note added in proof. Recently, a related paper by J. Martínez-Blanco *et al.* (Ref. 21) was published. The same system was studied by ARPES in detail, and discussion on the phase transition and coherence length of CDW based on their results is similar to ours. However, their conclusion as to the nature of the phase transition is quite contrary to ours, which is based on the results by several different approaches.

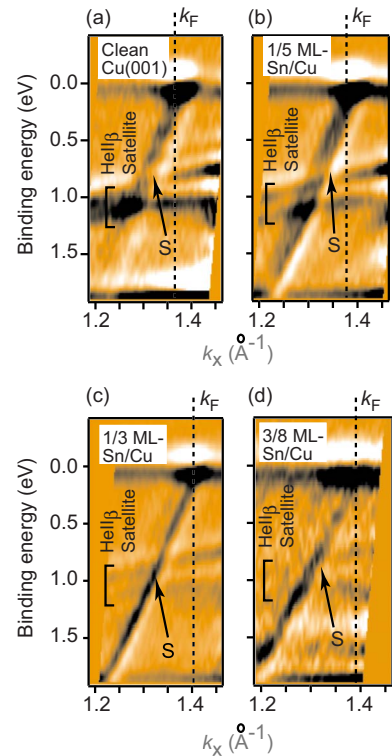


FIG. 6. (Color online) [(a)–(d)] Energy dispersion images of the surface resonance bands for clean Cu(001) and 1/5-, 1/3-, and 3/8-ML Sn/Cu(001) surface in the $\bar{\Gamma}\bar{M}$ direction of SBZ.

ACKNOWLEDGMENTS

The authors thank T. Okuda and A. Harasawa for their collaboration in the beam time at KEK-PF BL18A, and S. Shin, K. Ishizaka, and A. Shimoyamada for their collaboration in high-resolution ARPES experiments at the Institute for Solid State Physics, the University of Tokyo. The authors are also grateful to M. Yamada for fruitful discussion. Part of the present work was performed under the approval of the Photon Factory Program Advisory Committee (PF-PAC No. 2006G014).

APPENDIX: SURFACE RESONANCE BANDS DEPENDING ON TIN COVERAGE

Sn/Cu(001) system exhibits a variety of surface structures depending on the Sn coverage in the submonolayer region.^{8–11,19} Here, we briefly present the results of ARPES and discuss the electronic states for the 0-, 1/5-, 1/3-, 3/8-,

and 5/8-ML Sn/Cu(001) phases. The sample temperature during the measurements was set to 125 K for the 0-, 1/5-, 1/3-, and 5/8-ML Sn/Cu(001) phases. Concerning the 3/8-ML Sn/Cu(001) phase, the temperature was set to 425 K. Figure 6(a)–6(d) show the energy dispersions of the surface resonance bands for the clean Cu(001) and 1/5-, 1/3-, and 3/8-ML phases Sn/Cu(001) surfaces. No similar resonance band is observed in the same area of the k space for the $c(4 \times 4)$ surface with 5/8-ML Sn coverage. Unpolarized He II ($h\nu=40.82$ eV) radiation was used as photon sources for the ARPES measurement. The dispersions agree with the *free-electron-like* behavior. The surface resonance band for the clean surface reproduce the results of the previous band calculation.²⁰ It is found that the k_F of the surface resonance band shifts to the higher-wave-number side with increasing the Sn coverage. In addition, the effective mass of the electron of 0.5-ML Sn/Cu(001) is heavier than those of clean Cu and 1/5-, 1/3-, and 3/8-ML Sn/Cu(001).

¹R. E. Peierls, *Quantum Theory of Solids* (Clarendon, Oxford, 1955).

²A. Fröhlich, Proc. R. Soc. London, Ser. A **233**, 296 (1954).

³W. L. McMillan, Phys. Rev. B **16**, 643 (1977).

⁴T. Aruga, Surf. Sci. Rep. **61**, 283 (2006).

⁵J. Martínez-Blanco, V. Joco, H. Ascolani, A. Tejada, C. Quirós, G. Panaccione, T. Balasubramanian, P. Segovia, and E. G. Michel, Phys. Rev. B **72**, 041401(R) (2005).

⁶C. Binns and C. Norris, J. Phys.: Condens. Matter **3**, 5425 (1991).

⁷X. Gao, Y. M. Zhou, S. C. Wu, and D. S. Wang, Phys. Rev. B **66**, 073405 (2002).

⁸C. Argile and G. E. Rhead, Thin Solid Films **87**, 265 (1982).

⁹E. McLoughlin, A. A. Cafolla, E. AlShamaileh, and C. J. Barnes, Surf. Sci. **482-485**, 1431 (2001).

¹⁰K. Pussi, E. AlShamaileh, E. McLoughlin, A. A. Cafolla, and M. Lindroos, Surf. Sci. **549**, 24 (2004).

¹¹Y. Nara, K. Yaji, T. Iimori, K. Nakatsuji, and F. Komori, Surf. Sci. **601**, 5170 (2007).

¹²D. Sekiba, K. Nakatsuji, Y. Yoshimoto, and F. Komori, Phys.

Rev. Lett. **94**, 016808 (2005).

¹³D. Sekiba, Y. Yoshimoto, K. Nakatsuji, Y. Takagi, T. Iimori, S. Doi, and F. Komori, Phys. Rev. B **75**, 115404 (2007).

¹⁴F. M. Leibsle, C. F. J. Flipse, and A. W. Robinson, Phys. Rev. B **47**, 15865 (1993).

¹⁵H. Ellmer, V. Repain, S. Rousset, B. Croset, M. Sotto, and P. Zeppenfeld, Surf. Sci. **476**, 95 (2001).

¹⁶C. Cohen, H. Ellmer, J. M. Guigner, A. L'Hoir, G. Prévot, D. Schmaus, and M. Sotto, Surf. Sci. **490**, 336 (2001).

¹⁷S. M. Driver and D. P. Woodruff, Surf. Sci. **492**, 11 (2001).

¹⁸F. Komori, S. Ohno, and K. Nakatsuji, Prog. Surf. Sci. **77**, 1 (2004).

¹⁹A. A. Cafolla, E. McLoughlin, E. AlShamaileh, Ph. Guaino, G. Sheerin, D. Carty, T. McEvoy, C. Barnes, V. Dhanak, and A. Santoni, Surf. Sci. **544**, 121 (2003).

²⁰C. Baldacchini, L. Chiodo, F. Allegretti, C. Mariani, M. G. Betti, P. Monachesi, and R. Del Sole, Phys. Rev. B **68**, 195109 (2003).

²¹J. Martínez-Blanco, V. Joco, J. Fujii, P. Segovia, and E. G. Michel, Phys. Rev. B **77**, 195418 (2008).